Spranger, T., van Pinxteren, D., Reemtsma, T., Lechtenfeld, O.J., Herrmann, H. (2019):
2D liquid chromatographic fractionation with ultra-high resolution MS analysis resolves a vast molecular diversity of tropospheric particle organics
Environ. Sci. Technol. **53** (19), 11353 - 11363

https://doi.org/10.1021/acs.est.9b03839

2-D liquid chromatographic fractionation with ultra-high resolution MS analysis resolves a vast molecular diversity of tropospheric particle organics

TOBIAS SPRANGER[1], DOMINIK VAN PINXTEREN[1], THORSTEN REEMTSMA[2], OLIVER J. LECHTENFELD[2,3], HARTMUT HERRMANN[1]*

[1]Atmospheric Chemistry Department (ACD), Leibniz Institute for Tropospheric Research (TROPOS), Leipzig, 04318, Germany

[2]Department of Analytical Chemistry, Helmholtz Centre for Environmental Research - UFZ, Leipzig, 04318, Germany

[3]ProVIS – Centre for Chemical Microscopy, Helmholtz Centre for Environmental Research - UFZ, Leipzig, 04318, Germany

Manuscript for re-submission to
Environmental Science and Technology
August 20th, 2019

Abstract

A 2D-liquid chromatographic fractionation method was combined with direct infusion electrospray ionization Fourier transform ion cyclotron resonance mass spectrometry to better resolve the high complexity of organic material in atmospheric particles. The number of assigned molecular formulas increased by a factor of 2.3 for the fractionated sample (18144) compared to a bulk sample analysis without fractionation (7819), while simultaneously allowing the identification of 71240 isomeric compounds. Accounting for these isomers has an impact on means and distributions of different descriptive sample parameters. More than 15000 compounds were exclusively identified in the fractionated sample providing insights regarding the formation of organosulfates, reduced N-containing compounds and polyaromatic compounds. Further, a new method for assigning organonitrates and poly-organonitrates based on Kendrick mass defect analysis is presented.

The current study implicates that analytical separation leads to much more detailed insights into particle organics composition, while more commonly applied direct infusion MS studies can strongly underestimate composition complexity and lead to biased assignments of bulk organic properties. Overall, particle organics composition is far more complex than previously shown, while separation through better chromatographic techniques helps to understand formation processes of atmospheric particle constituents.

Introduction

Atmospheric aerosol particles are a complex mixture of inorganic ions, mineral dust, elemental carbon and organic compounds. Elucidating the composition of the organic carbon (OC), which can contribute up to 70% of the particulate mass (PM)[1], is especially difficult with thousands of different constituents, often classified into water-soluble (WSOC) and water-insoluble organic carbon. Most of the OC has not been characterized on a molecular level[2], despite its possible influence on microphysical particle properties[3-8], human health[9, 10], radiation and climate[11], and ecosystems.[11] A large fraction (20-80% of WSOC) of unknown substances is often referred to as humic-like substances (HULIS).[12-14] However, HULIS is only operationally defined and the observed molecular composition can be heavily influenced by the applied solid phase extraction (SPE).[15-19] While the term HULIS is still in use, it seems more appropriate to refer to this fraction of organic aerosol as $\mathrm{WSOC_{SPE}}$, similar to terms used for different fractions of one particular SPE method[20, 21] or to distinguish between extracts of the same samples from different SPE methods.[19]

While methods have been developed to analyze individual compounds or compound groups, the high complexity of $\mathrm{WSOC_{SPE}}$ samples makes analytical methods yielding more comprehensive molecular information of bulk mixtures more appealing. Lately, UHR-MS and particularly Fourier-transform ion cyclotron resonance mass spectrometry (FT-ICR MS) has been used to elucidate the composition of $\mathrm{WSOC_{SPE}}$ and OC on a molecular level, as it allows the measurement of thousands of signals simultaneously.[22-29] Due to the ultrahigh mass resolution and accuracy of FT-ICR MS instruments, an explicit molecular formula (MF) can be assigned to most of the signals,[30] also including heteroatoms like N and S.[31] However, one MF can represent many isomeric compounds, i.e. molecules with the same elemental composition but different structures and hence different properties.[32] Additionally, it is known that the mass spectral representation of a sample heavily depends on the applied ionization method and the relative ionization potentials of the samples molecular species.[28, 33, 34] Finally electrospray ionization (ESI) is prone to strong matrix effects leading to suppressed or enhanced response factors and thus to an even more biased view on the sample composition.[35-37]

The vast majority of studies applying UHR-MS on atmospheric samples use direct infusion[22-28], where there is no separation of compounds prior to the injection of the sample solution into the mass spectrometer. For measurements with an Orbitrap mass spectrometer, providing lower mass resolution than FT-ICR MS, one-dimensional liquid chromatography (LC) is also applied.[32, 38, 39] It has been shown that the isomeric complexity of natural organic matter by far exceeds achievable 1D-chromatographic resolution.[40] Hence two-dimensional chromatography (2D-LC) is needed to better resolve the complexity of $WSOC_{SPE}$.[41, 42] As a first step towards 2D characterization, a 2D-LC fractionation method combining size-exclusion chromatography (SEC) and RP-HPLC was recently developed in our laboratory.[43] The resulting 55 fractions highlight distinct differences in the UV-absorption between samples from the same sampling location at different seasons and meteorological conditions.[43] However, chemical information like MF were lacking in that study. Fractionated $WSOC_{SPE}$ samples in combination with UHR-MS measurements might have a high potential for revealing a more detailed chemical composition than the commonly applied bulk sample analysis. Therefore, in the present study a comparison was undertaken for the analysis of atmospheric particle samples from the TROPOS research station (Melpitz, Germany 51°32′N, 12°56′E) with 2D-LC fractionation combined with FT-ICR-MS on the one hand and the measurement of the bulk samples with direct infusion FT-ICR-MS on the other hand.

Materials and methods

Particle sampling and sample preparation

Five atmospheric particle samples were collected at the TROPOS research station in Melpitz[44] (45 km northeast of Leipzig; 51°32′N, 12°56′E) during the summer of 2014 using a Digitel DHA-80 high-volume filter sampler over 24 h sampling time (Table S1). Particulate matter with an aerodynamic diameter of less than 10 µm (PM10) was collected on preheated (24 h at 105 °C) quartz fiber filters (Munktell MK 360, Sweden). $WSOC_{SPE}$ was isolated by extracting the filter with ultrapure water (Milli-Q, Millipore, Schwalbach, Germany) followed by a SPE using an Oasis HLB 3 cm^3 cartridge (Waters, United States, sorbent mass 60 mg). The used protocol and its limitation regarding the loss of very hydrophilic compounds are described in detail in the supporting information. $WSOC_{SPE}$ was then separated into 55 fractions using a 2D-LC method published earlier.[43] Briefly, in the first dimension $WSOC_{SPE}$ is fractionated into five molecular size fractions on a PL aquagel−OH 20 column (Agilent; 300 mm × 7.5 mm; 8 µm particle size) and in the second dimension into eleven fractions with different polarity on a C-18 Atlantis column (Waters; 2.1 mm× 100 mm; 3 µm particle size) utilizing a spiked gradient.[43] The individual fractions were collected, evaporated to dryness and stored at -18°C. Just before the MS measurements, they were reconstituted in 1:1 (v/v) water: methanol and diluted to equal UV-absorbance at 254 nm, resulting in expected similar concentrations of organics. In addition to the aerosol sample, a field blank was taken and an analogous procedure was applied (including transport to field site, staying inside the Digitel, transport to laboratory, weighing), with the difference, that all SEC fractions were collected together. Accordingly, the number of blank measurements was reduced to more feasible 11 method blanks, one for each individual RP-HPLC fraction, while still being representative for the sample treatment. The sample treatment includes multiple reactive species, such as ammonia, formic acid or methanol, which potentially could alter the composition in the sample preparation and chromatographic process. To check the influence of such potential artifact, additional quality control measurements with standard substances resembling the functional variety of atmospheric compounds and with Suwannee River Fulvic Acids (SRFA) were performed.

FT-ICR MS measurements

In total, 38 fractions of sample 1 (Figure S1) and two fractions of samples 2-5 were analyzed using negative electrospray ionization and an FT-ICR-MS (Bruker) located at the ProVIS Centre for Chemical Microscopy within the Helmholtz Centre for Environmental Research, Leipzig. Sample 1 was analyzed comprehensively to demonstrate the possible advantages of such an extensive sample preparation, while samples 2-5 were utilized as quality controls to study the reproducibility between different atmospheric particle samples from the same location with similar meteorological conditions. Further details about the instruments, measurement details and explanations for the choice of the fractions measured are presented in the supporting information. Mass peaks were considered if the signal/noise (S/N) ratio was greater than four and all mass peaks present in the instrument blank and in the method blanks mentioned earlier were removed from the final mass list (8371 peaks). This conservative approach partially even removes MF identified as secondary organic aerosol tracers like $C_{10}H_{14}O_4$, $C_7H_{10}O_4$ and $C_7H_{12}O_7S$[45], because they were found in one of the blanks. MF were assigned to mass peaks in the range *m/z* 150 - 750 allowing for elemental compositions $C_{1-60}{}^{13}C_{0-1}H_{1-122}N_{0-5}O_{1-40}S_{0-1}{}^{34}S_{0-1}$ with an error range of ±0.5 ppm following the rules previously described.[46, 47] The consideration of high numbers of N-atoms (N_3-N_5) is necessary for atmospheric aerosol particle sample, as such compounds were identified in recent studies.[48, 49] Further details to the MF assignment as well as the utilized molecular parameters are described in the supporting information.

Result and discussion

Improved molecular picture from bulk vs. fractionated comparisons

In the following the results of bulk injection and fractionated sample measurements of sample 1 are compared. Differences between the two approaches are described with regards to the numbers of assigned molecular formulas and compounds, the general size and compounds distribution as well as different molecular parameters like double bond equivalent (DBE), aromaticity equivalent, carbon oxidation state and compound volatility.

Number of molecular formulas

The bulk sample of the $WSOC_{SPE}$ – solution was measured with direct infusion and 7819 molecular formulas (MF) were assigned to the observed mass signals, each representing a unique elemental composition. To the authors' knowledge, this is a higher number of assigned MF than in any other bulk sample study of $WOSC_{SPE}$ and multiple reasons do account for this. The molecular formula calculation parameters of the present study allow for a high number of compounds (low S/N, up to N_5 molecules) and the WSOC concentration of the bulk sample based on UV-absorption at 254 nm of the extract was high. Moreover, the sample has a broad distribution of the UV-absorption, indicating a high diversity of molecules (S1).

For comparison with the bulk sample, the mass spectra of the individual measured 2D fractions from the same $WSOC_{SPE}$ – solution were combined to a Sum-of-all-Fractions (SoaF) integrated sample. Even with the applied very conservative blank handling, 18144 MF can be assigned to the exact masses observed for SoaF with 6464 MF in common with the bulk measurement and 11680 additional ones which likely were suppressed in the bulk measurements. 1355 MF are not detected in the SoaF sample but in the bulk sample. These MF are detected with a lower S/N (17.5 compared to 39.9 of the full bulk sample) predominantly at m/z > 500 (Figure S11). Possibly, those compounds are already efficiently ionized, so that the increase in efficiency in the fractionated measurements is not sufficient to compensate for the separation of isomers into many different fractions for these MF. Furthermore, some MF might be missing because 16 fractions with estimated very low carbon concentrations out of the total 55 sample fractions were not measured. In addition, despite careful sample processing, losses during the fractionation method cannot be ruled out completely.

Number of isomeric compounds

Out of the 18144 MF detected in the SoaF sample, 10561 MF were present in single, but different, fraction only, while the remaining 7583 MF were found in at least 2 up to a maximum of 34 fractions (mean number of fractions = 8, 5th percentile = 2, 50th percentile = 5 and 95th percentile =23). MF with m/z > 500 were found in significantly fewer fractions than MF with smaller m/z (Figure S12). At the same time, the 10561 MF present in only one fraction contain a high number of compounds with m/z > 500 (Figure S13). It is likely that MF with higher m/z are less often detected in different fractions, due to their lower overall signal intensity and thus quick dilution to non-detectable levels upon fractionation (see also discussion of the bulk sample).

The detection of the same MF in different fractions is assumed to mainly originate from different isomers being resolved into different fractions in the chromatographic separation. Another reason could be poor separation efficiency for a given compound leading to its presence in two or even more adjacent chromatographic fractions, which is discussed with its implications for the number of isomers in SI section ‘Different data treatment options for the fractionated sample’. Given the expected high number of isomers in atmospheric aerosol particles[32, 39, 50], however, the detection of a MF in one fraction is defined as an individual compound in the following. With this assumption 71240 different compounds are detected in the SoaF sample, compared to 7819 compounds distinguishable in the bulk sample. It is important to note that the resulting number of total compounds represents a lower estimate only, as any MF can always represent a number of different isomeric compounds, regardless of its appearing in one or multiple fractions. More accurate estimations could only be obtained by strongly increasing the chromatographic separation of the compound mixture.

Out of the 71240 different compounds, 79% are isomers of MF that are also detected in the bulk sample. Further 21% (15212) are newly identified compounds, whose MFs are not detected in the bulk sample. In the following parts the distributions of the compounds and mean properties are discussed for the bulk and SoaF sample, as well as the newly identified compounds.

Size and compound group distributions

The 7819 bulk sample MF are separated into 26.3% CHO-, 50.4% CHNO-, 9.8% CHOS and 13.5% CHNOS-compounds broadly distributed over the whole m/z-range (Figure 1A). These results are comparable in terms of m/z and compound group distribution from UHR-MS measurements of aerosol constituents done in the past[22, 24-26, 28, 39, 51-53], especially those including signals with lower intensities, resulting in a more prominent CHNO-fraction.[22, 26, 53]

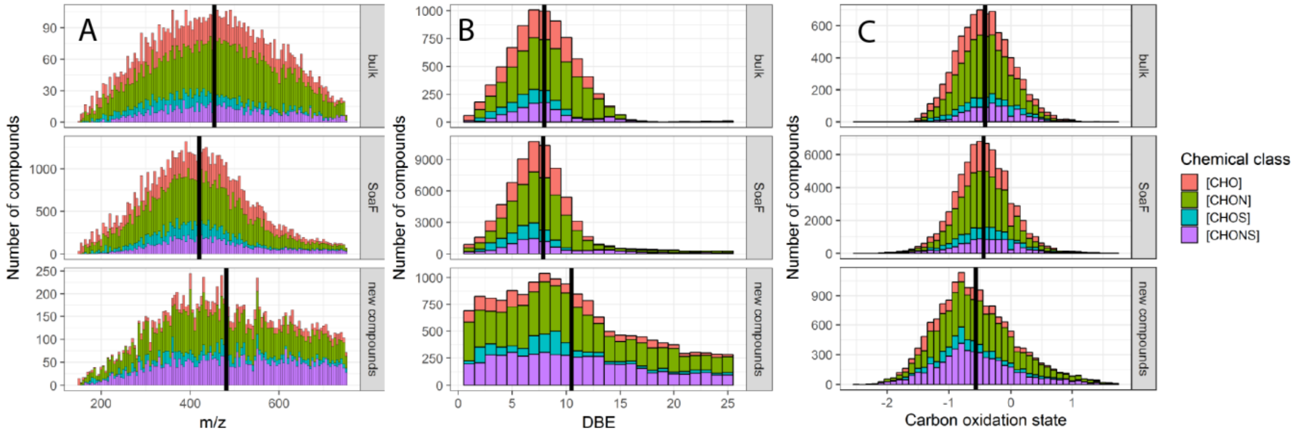

Figure 1: Histogram of the m/z (A), DBE (B) and $\overline{OS_c}$ (C) of the compounds found in the bulk sample, the integrated fractionated sample SoaF and the newly identified compounds, identified only in the SoaF sample. Color indicates the compound groups CHO, CHNO, CHOS, CHNOS. The black line indicates the respective mean value.

The measurements of the fractionated sample (SoaF) reveal huge differences compared to the bulk sample. The 71240 detected compounds in SoaF can be separated into 27.3% CHO-, 47.1% CHNO-, 11.3% CHOS- and 14.2% CHNOS-compounds. Compared to the 7819 detected compounds in the bulk sample, this is an increase of 910% in the number of compounds, while the distribution over the four molecular formula classes is similar. Figure 1A shows that SoaF has a significantly higher fraction of medium sized compounds (300-550 m/z) and a slightly lower average m/z compared to the bulk sample.

The 15212 newly identified compounds are evenly distributed over the entire mass range for m/z > 300, while compounds of lower molecular weight are less prominent (Figure 1A). They only contain a small fraction of CHO-compounds (11.9%), but many heteroatom containing compounds (45.3% CHNO, 10.1% CHOS, 32.6% CHNOS).

Figure 1B shows a very similar distribution of the DBE for the compounds in the bulk and SoaF. The newly identified compounds are detected at higher DBE, indicating a higher degree of aromaticity. Further, the calculation of the aromaticity equivalent[54] reveals a large fraction of newly identified polyaromatic compounds (35.1%). It is likely that the 2D-LC fractionation reduces the suppression of these compounds which are difficult to ionize in electrospray ionization, so that in contrast to the bulk sample, even low intensity compounds (mean S/N = 6.3) can be detected.

Carbon oxidation state $\overline{OS_c}$

To characterize and compare complex organic aerosol mixtures, the calculation of the carbon oxidation state $\overline{OS_c}$ was established by Kroll et al. in the past years.[55] Based on the assignment of the MF the $\overline{OS_c}$ can be calculated (eq. S4 in supporting information) and compared for the bulk and fractionated sample.

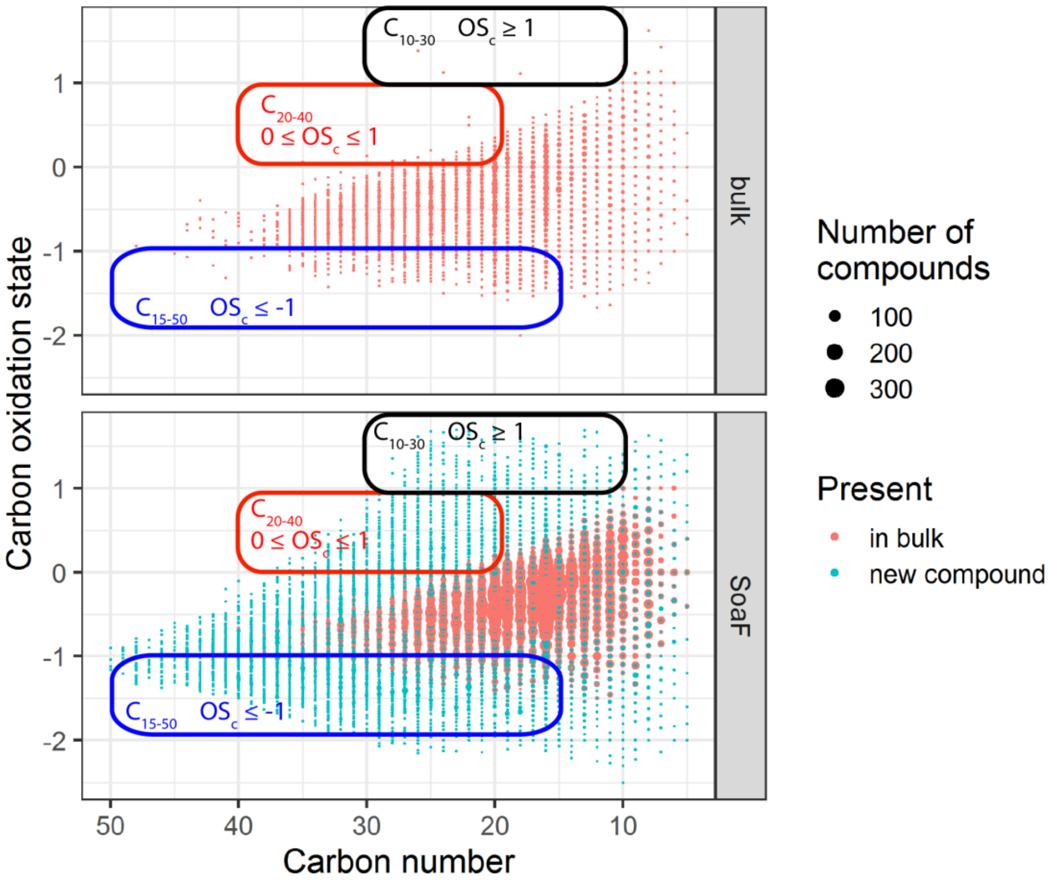

Figure 2: Location of the compounds in the carbon oxidation state – carbon number space for the bulk (top) and SoaF (bottom). For the SoaF sample the color indicates, whether a compounds newly identified in the fractionated sample or also present in the bulk sample. The blue, red and black areas highlight the largest differences between both samples and are further discussed in main manuscript.

The mean $\overline{OS_c}$ of ~ -0.4 as well as the unimodal distribution (Figure 1C) does not differ between the bulk and SoaF sample and is within the wide range of mean values from -2.0 to 0.9 of other ambient samples.[55, 56] The $\overline{OS_c}$ vs. carbon number space (Figure 2) reveals further features of the fractionated measurement. The newly identified compounds cover a much larger range of $\overline{OS_c}$ than the bulk compounds. On the one hand, there are compounds with $C_{>15}$ with $\overline{OS_c} < -1$, for which a lower ionization efficiency can be expected and which are only detected after the reduction of ion suppression effects by the fractionation. On the other hand, there are more oxidized compounds present, one group with C_{20-40} and $0 \leq \overline{OS_c} \leq 1$, which could possibly be oligomers of smaller molecules with similar $\overline{OS_c}$ [55, 57], and another group of C_{10-30} and $\overline{OS_c} \geq 1$. The finding of the latter group is quite remarkable, as these compounds were suggested to be absent in the atmosphere.[55] The calculation of $\overline{OS_c}$ requires estimations of the oxidation states of sulfur and nitrogen. Therefore the calculation can differ strongly for compounds with heteroatoms depending on the estimated oxidation state (see also section 'Discussion of the calculation of the carbon oxidation state' in the SI). Nevertheless, the newly found compounds lead to a much more diverse distribution in the $\overline{OS_c}$ vs. carbon number space compared to the bulk sample. This could indicate currently unknown and undiscovered formation or aging processes of WSOC in atmospheric aerosol particles.

Relative elemental composition

For a better understanding of the compounds present in the sample, utilizing Van-Krevelen (VK) diagrams is very useful.[58] These diagrams display molecular formulas on an O/C vs. H/C -plane. In the literature, a 3rd dimension, either coded with different colors or dot sizes, is often used to present the compound intensity. Since ESI derived mass peak intensities for complex mixtures are not a good measure for concentrations due to very different ionization efficiencies, in this study the 3rd dimension is used to indicate the number of compounds with the same ratios instead.

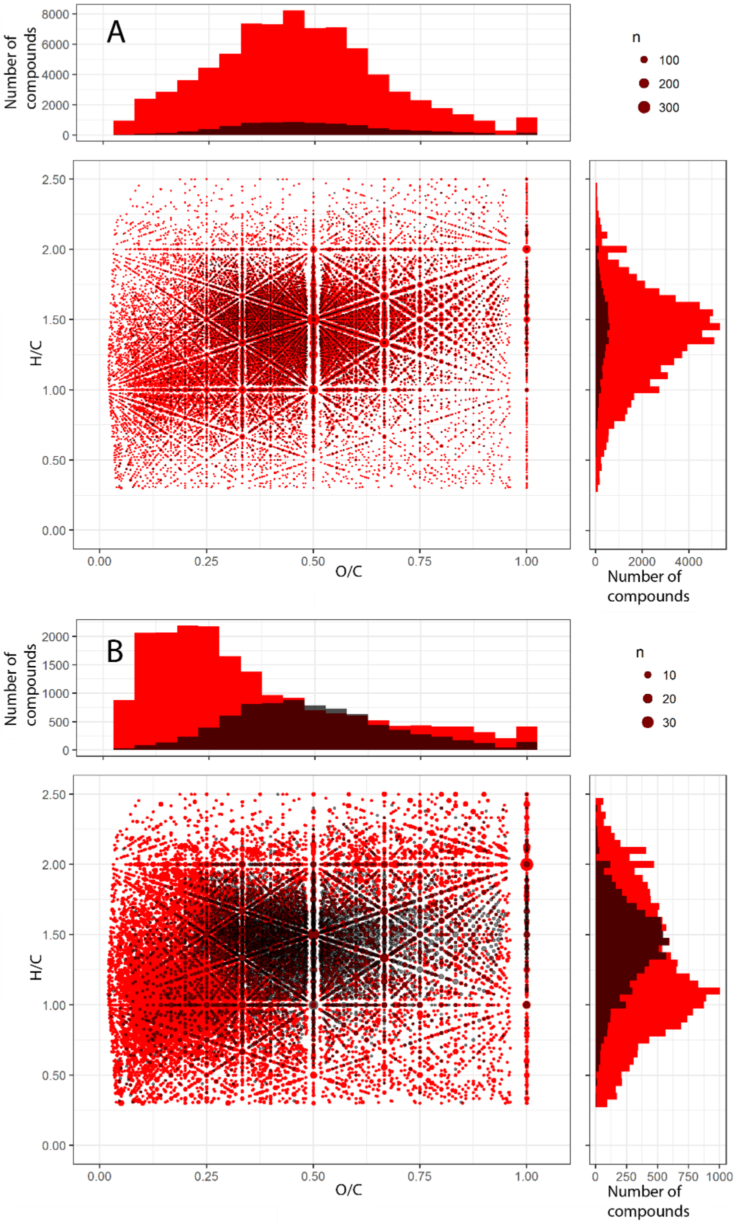

Figure 3: Van-Krevelen Diagram of all compounds detected in the bulk sample (black) and A) all compounds in the fractionated sample (SoaF in red) or B) all newly identified compounds (those without bulk MF; in red). Dot size illustrates the number of compounds with the same ratios, while the histograms illustrate the one-dimensional O/C and H/C distribution. Only MF with H/C ≤ 2.5 are shown for a better visibility (100 MF are not shown). Note that slight color distortions arise from overlapping transparent points.

Figure 3A shows the VK diagram for all compounds present in the bulk (black) and SoaF (red) samples. The compounds in the bulk sample are mainly located in the center at O/C [5th percentile = 0.22, 50th percentile = 0.48, 95th percentile = 0.86] and H/C [0.88, 1.43, 1.89]. This distribution is similar to those reported in the literature for bulk samples of continental aerosol particles or other natural organic matter.[26, 31, 59-63] For other types of aerosol particles, this distribution can differ, especially for highly polluted areas the distribution is shifted towards lower O/C and H/C-ratios due to the increased presence of aromatic and polyaromatic compounds as well as more nitrogen containing compounds.[26, 28, 39] SoaF shows compounds over the whole plot area centered at O/C [0.17, 0.47, 0.83] and H/C [0.80, 1.42, 1.93] with a higher amount of compounds in the low O/C-ratio part. Since the majority of SoaF compounds are isomers of bulk compounds, the differences are more distinct when comparing the bulk sample with only the newly identified compounds (Figure 3B). They are strongly shifted towards lower O/C- [0.07, 0.33, 0.90] and lower and broadly distributed H/C- ratios [0.52, 1.38, 2.14], thus it can be expected, that these compounds are less ionizable and thus suppressed in the bulk sample. Also very low concentrations of individual compounds are possible, especially for the polyaromatic compounds often measured in highly polluted areas. The distribution of compounds in the VK-diagram separated into the different groups (CHO, CHOS, CHNO, CHNOS) is similar to the general distribution of the newly identified compounds (Figure S14-S19). For all groups the majority of compounds is detected at lower O/C-ratio than the compounds of the bulk sample. Further, the CHNO- and CHNOS-compounds show a higher diversity of O/C- and H/C-ratios compared to the CHO- and CHOS-compounds.

Summarizing the general comparison, the dataset shows that a large number of compounds are not detected when only bulk measurements are performed. The sample fractionation prior to the UHR-

MS measurements leads to reduced ion suppression in the ESI process and a separation of isomeric compounds and thereby drastically increases the number of detected compounds, thus leading to a more complete picture of the WSOC_{SPE} composition. The more complete molecular composition, in turn, impacts the calculation of chemical and physical particle properties (Table S2), like the carbon oxidation state, DBE or volatility (for more details also see "Discussion of the calculated volatility C_0" in the supporting information). Even though their accurate calculations would require the consideration of concentrations of all compounds in the mixture, which are not available, the discussion of distributions and number-based mean values in the sections above already indicate that a better molecular resolution can lead to different calculated sample properties.

2D-distribution of various sample parameters

The different MS-parameters used for the comparison of bulk and fractionated sample, also show distinct distributions in the 2D-space of the LC-fractionation method and are presented in Figure 4 and Figure S9. Mean values for the different parameters are shown for individual fractions and plotted as heat maps in the polarity vs. size space of the 2D separation. Axis labels, logP for polarity and m/z for size, are based on calibrations performed with standard solutions.[43] The calibrated m/z ranges of the SEC dimension do not represent sharp boundaries, but are rather meant to indicate a broad tendency towards more smaller or larger sizes in the different fractions. In fact, broad MS spectra were observed for all SEC fractions and mean observed m/z were between approx. 400 and 500 (Figure S9 D). This is mainly because SEC does not separate by molecular weight, but molecular size, or more precisely hydrodynamic radii of analytes and their solvent shell. Molecular weight and size only correlate in very similar molecules, e.g. homologous series, but can differ strongly in dissimilar molecules. The size separation is apparent in the aromaticity of the different fractions. Fractions associated with larger-sized molecules contain the highest amount of polyaromatic compounds (Figure 4C), those with medium-sized molecules contain more monoaromatic compounds (Figure 4B) and fractions with small molecules mostly contain non-aromatic compounds. Accordingly, the mean DBE decreases and the mean H/C ratio increases in smaller-sized molecules (Figure S9 A&C).

Another clear trend can be seen for the $\overline{OS_c}$ and the O/C-ratio (Figure 4A, S9 B). For both parameters, the highest mean values can be found in the fractions associated with the highest polarity (lowest logP) and decreasing with lower polarity. Furthermore, a small increase in mean molecular weight and H/C-ratio can be observed with decreasing polarity. Those results match the separation mechanism on the column mostly based on dipol-dipol and ion interactions of analytes with the mobile phase and on hydrophobic interactions with the stationary phase. The 2D-distributions shortly discussed here provide new insights on how different sample properties are distributed within the broad polarity vs. size space, which will be further exploited in future studies. In the present study, we rather focus on the additional sample complexity our method was able to resolve and how this new information can help when studying different organic compound classes and their respective mechanisms of formation.

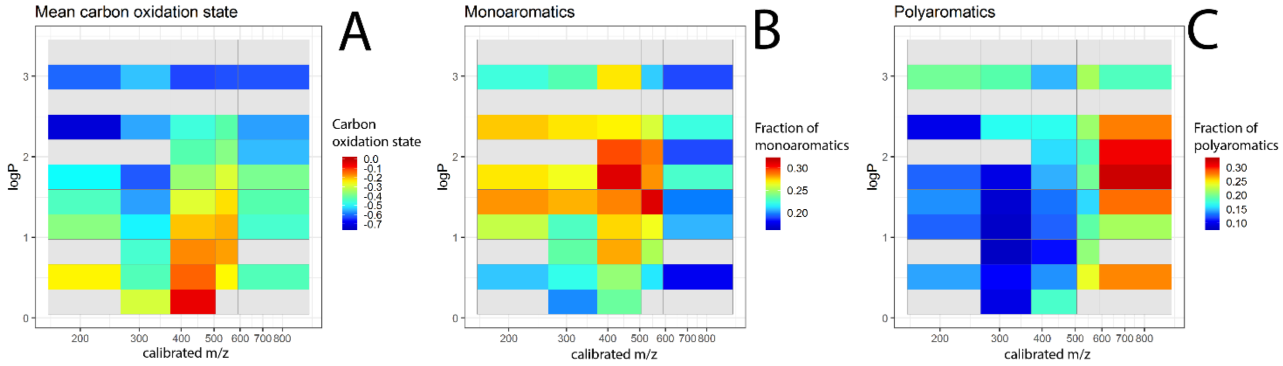

Figure 4: 2D-heat maps of mean $\overline{\mathrm{OS}_{\mathrm{c}}}$ (A) and the fraction of monoaromatic (B) and polyaromatic (C) compounds in each fraction.

Reproducibility and representativeness of the FT-ICR MS-measurements

The previous sections highlighted a large gain in detected compounds for particle organics, when analyzed as a fractionated sample compared to a bulk sample analysis. To assure the reproducibility of those measurements, SRFA was measured with six repeated injections. The vast majority of MF (~1800 MF) are detected in all six repetitions, while only ~120 MF are unique in each measurement. Very similar results with 94% of signals detected in all repetitions are also found for two individual fractions of sample 3 (see SI "Discussion of quality assurance and control measurements", Figure S4), so that a good reproducibility of fractionated sample measurements is given with the applied MS-settings.

To assure that the newly identified compounds are not artifacts, generated during the extensive sample treatment, SRFA and a mixture of standard substances (Figure S5) were measured at three different times during the sample treatment. For SRFA the same distribution of MF as for the six repeated injections is found (Figure S6). Similarly, for the mixture of standard substances no reactions occurred during the different sample preparation steps, as the intensity and S/N of the individual compounds remained constant (Figure S5). In conclusion, this demonstrates that no significant artifact formation takes place during sample preparation, which means the high number of additional MF are most likely detected due to changes in the ionization efficiency and reduced ion suppression effects.

In the previous sections, sample 1 was analyzed extensively. To study how representative this sample is in a larger atmospheric context, two fractions of four additional aerosol samples were analyzed. The variability in the molecular composition is higher than for repeated injections of the same sample (Figure S7 and S8). Sample 1 and 4 show the highest amount of unique MF (~900-1500), while sample 2, 3 and 5 show a more similar composition with only 100-300 unique MF each. For the distribution of the various sample parameters a similar trend is identified, however the variability in the mean values of all parameters is much smaller for the same 2D-fractions in the five different aerosol samples compared to the variability within different fractions of sample 1 (Figure 4, more details in SI “Discussion of quality assurance and control measurements”). In summary, looking at individual assigned MF, there is still the possibility for a high number of unique MF in the same fraction of different samples, which is expected due to natural variability. Overall, however, after the 2D-LC fractionation, the compounds in the same fraction from several samples taken during similar atmospheric conditions show a high similarity in terms of mean values and overall distributions. Those conclusions are currently based on a small number of samples due the large amount of manual work in the fractionation method and the data acquisition and processing. To facilitate sample analysis, the LC-MS method should be further developed to an online-2D-LC-MS method in the future. Additional improvements and automation in the data acquisition and MF assignment would further increase the accessibility to a broader user base.

Implications for different organic particle compound classes

The newly identified compounds, which are present in the SoaF sample, but not in the bulk one, provide new information about the sample compositions that can help to reveal new or substantiate previously suggested emission or formation pathways for tropospheric organic particle constituents. Therefore, these newly identified compounds are further discussed in the following parts and compared to findings for the compounds from the bulk sample and SoaF.

Organonitrates

In the present dataset most compounds are assigned as CHNO-compounds (45% of newly identified, 47% of SoaF and 50% of compounds in the bulk) distributed over a wide range of O/C- and H/C-ratios. The newly identified compounds contain a larger fraction of compounds with multiple nitrogen atoms as compared to the bulk sample (20% CHN_1O, 26% CHN_2O, 23% CHN_3O, 18% CHN_4O and 13% CHN_5O for newly identified compounds compared to 56% CHN_1O, 31% CHN_2O 7% CHN_3O, 4% CHN_4O, and 2% CHN_5O for the compounds detected in the bulk sample). Organonitrates $R\text{-}ONO_2$ likely contribute to these compound classes as they are known to be formed through the gas phase reaction of peroxy radicals with NO.[64] Additionally, nitrate radical chemistry [65] could as well lead to organonitrates. Further, aromatics, and especially phenols, can react faster than most other atmospheric species with nitrate radicals.[65] CHNO-compounds are often classified as organonitrates, just based on an elemental ratio of $O/N > 3$.[24, 28, 59] However, depending on the number of other oxygen-containing functional groups assumed to be present in the same compounds, a large uncertainty arises with respect to the fraction of organonitrates as well as other potential compounds like nitro-aromatics (for more details see supporting information section "Classification of CHNO-molecules"). In the present dataset between 83% (0 oxygen atoms in other functional groups) and <5% (12 oxygen atoms in other functional groups) of the CHNO-compounds could be classified as organonitrates (Figure S10).

A superior approach to identify CHNO-compounds is to analyze potential reaction products or precursors. It was shown that organonitrates can hydrolyze under atmospheric condition to an alcohol and nitric acid ($R\text{-}ONO_2 + H_2O \rightarrow R\text{-}OH + HNO_3$).[66] The detection of both MF ($R\text{-}ONO_2$ and R-OH) is an indication for the assignment of an organonitrate that improves over assignments based on O/N only. We emphasize that the actual structure of the MF cannot be derived from the MS-measurements alone. It should also be noted that the $R\text{-}ONO_2$ hydrolysis reaction might, to some extent, occur during the sample preparation. For 69% of the CHNO-compounds in the bulk sample, 67% of the CHNO-compounds in the fractionated sample and 28% of the newly identified CHNO-compounds the respective alcohol of the organonitrate was detected. Further, this approach opens up the possibility to assign poly-organonitrates, compounds with multiple $R\text{-}ONO_2$ units, for the first time in environmental science. To identify and illustrate these poly-organonitrates a Kendrick mass defect (KMD, eq. S6) analysis is a helpful tool.[67] All molecules, which only differ in the number of certain structural elements, here ($-H+NO_2$), have the same Kendrick mass defect and thus can easily be identified as hydrolyzed or non-hydrolyzed organonitrate compounds (Figure 5). This calculation reveals 21% of the CHNO-compounds in the bulk sample, 18% of the CHNO-compounds in the fractionated sample and 16% of the newly identified CHNO-compounds can be assigned to poly-organonitrates. In some cases even full series are detected, e.g. from $C_{15}H_{13}N_5O_{15}$ with five organonitrate groups down to the fully hydrolyzed compound $C_{15}H_{18}O_5$ with all intermediate steps. While the CHO and the N_1-N_3 compounds are also detected in the bulk sample, $C_{15}H_{14}N_4O_{13}$ and $C_{15}H_{13}N_5O_{15}$ are only detected in the fractionated sample (Figure 5), again indicating the benefits of the fractionated measurements. The results indicate that organonitrates are likely the most abundant CHNO-compounds number wise and poly-organonitrates are also an important contributor to the $\mathrm{WSOC_{SPE}}$ composition. However, for one-third of the CHNO-compounds present in the bulk and SoaF sample and two-thirds of the newly identified CHNO-compounds other reduced N-containing functional groups must be present. Heteroaromatics are a likely contributor, as 43% of the newly identified CHNO-compounds are polyaromatic and 22% are monoaromatic. 25% of the newly identified CHON-compounds are non-aromatic and no organonitrate functionality (based on the KMD analysis) is found for those. Compounds similar to larger amines generated by the reaction of α-pinene with O_3 in the presence of dimethylamine[48] could explain those (for more details see “Discussion on reduced N-containing compounds” in the supporting information).

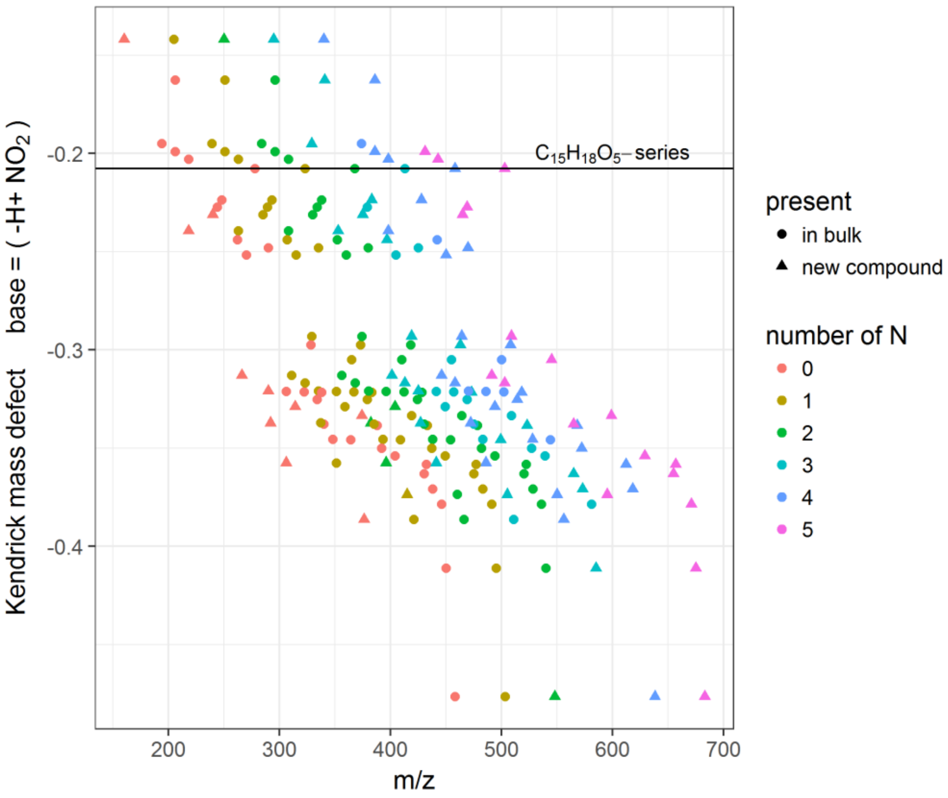

Figure 5: Kendrick mass defect plot for series of hydrolyzed organo-nitrates ($R\text{-}ONO_2 + H_2O \rightarrow R\text{-}OH + HNO_3$) for the compounds of the SoaF sample. For a better visibility only series with at least five different MF (with different m/z) are shown. Dots indicate that the compounds is also detected in the bulk sample, triangle indicates that the compound was only detected in the fractionated sample (newly identified compounds). The color scale shows the number of N-atoms per compound, thus the number of organo-nitrate groups. The black line highlights one full series from $C_{15}H_{18}O_5$ to $C_{15}H_{13}N_5O_{15}$.

Organosulfates

Organosulfates ($R\text{-}OSO_3$) represent another large group of relevant compounds in organic aerosol particles of strong interest in atmospheric chemistry since more than a decade. Most CHOS-compounds are generally attributed towards organosulfates in the literature[28, 29, 32, 60, 68-72], although it should be noted that other functional groups like sulfonate [73]($R-SO_3$) or sulfonyl ($R-SO_2-R$) groups or even reduced sulfur groups can form important sulfur-containing organics contributing to the CHOS group. The compositional similarity of these functional groups introduces a large uncertainty if organosulfates are assigned just based on elemental ratios, same as for the CHNO class. However, a precursor-product analysis via KMD[74] as performed for the organonitrates is also possible for the potential organosulfates. A known formation pathway of organosulfates is through epoxide precursors from the oxidation of mono- and sesquiterpenes.[75] In this pathway, the nucleophilic addition of sulphate ions is competing with the addition of water leading to either an alcohol (R-OH) or the organosulfates ($R-OSO_3H$). If the epoxide pathway is important for the organosulfates formation, both the alcohol as well as the organosulfate, should be present in the sample.[59, 76] Further, organosulfates can also be hydrolyzed under atmospheric condition, although slower than organonitrates, forming , again, the same alcohol (R-OH).[77] For the newly identified CHOS-compounds 852 alcohol-organosulfates-pairs can be identified (Figure S20) potentially explaining 48 % of all newly identified CHOS-compounds. Recently a different formation pathway for organosulfates was suggested, were SO_2 can directly react with double bounds to form new sulphur containing species in the atmosphere.[78] This could also be a relevant formation pathway for the newly identified compounds, as the main product of the reaction of oleic acid ($C_{18}H_{34}O_2$) and SO_2 is a cyclic organosulfates[78] and its MF $C_{18}H_{34}O_6S$ is actually found in the present dataset. Other CHOS-compounds could also be explained by similar reactions of SO_2 with poly-unsaturated fatty acids like linolenic acid ($C_{18}H_{30}O_2$) and linoleic acid ($C_{18}H_{32}O_2$), which would be reacting to the cyclic organosulfates $C_{18}H_{30}O_6S$ and $C_{18}H_{32}O_6S$, with both these MFs present in the dataset. For the newly identified CHOS-compounds 578 precursor-product-pairs ($C_xH_yO_z$ and $C_xH_yO_{z+4}S_1$) can be identified (Figure S21) possibly explaining 35 % of all newly identified CHOS-compounds. There is also an overlap of 477 organosulfates compounds, which can be explained by both the epoxide pathway and the addition of SO_2 to a double bond as both precursor-product-pairs are present.

Similar results to those of pure organosulfates and –nitrates are also found for nitrooxy-organosulfates[24, 32, 59, 63] and other CHNOS-compounds. For the bulk and SoaF sample ~40% of the CHNOS-compounds can be identified as nitrooxy-organosulfates, while for the the newly identified CHNOS-compounds only 12% can be explained as such (for more details see "Discussion on nitrooxy-organosulfates" in the supporting information).

Polyaromatic compounds

Another large fraction (~35%) of the newly identified compounds can be attributed to polyaromatic substances, either condensed or linear combined ones. In the atmosphere, polycyclic aromatic hydrocarbons (PAHs) are well-known particle constituents, which are usually not measured in the aqueous particle phase[79]. Through atmospheric oxidation and functionalization it is likely that these compounds become polar enough to partition in the aqueous phase. In the present study, the potentially oxidized PAH's are detected at O/C [0.05, 0.22, 0.63] and H/C [0.39, 0.90, 1.41]. PAHs are known to have negative impact on human and ecosystem health[9, 79, 80] and their oxygenated and water soluble derivatives could further increase the negative impact of this compound family. Most polyaromatic compounds in the present $WSOC_{SPE}$ sample contain nitrogen (~80% CHNO or CHNOS), thus the oxidation with nitrate radicals seems to play an important role for the PAH oxidation.[65, 79, 81] Reduced nitrogen and hetero aromatic compounds, like pyridine- and imidazole-like structures[82], might be important to explain further large fractions of the polyaromatic compounds.

For sulfur containing polyaromatic compounds, also organosulfates can be considered. Recently it was shown, that aromatic organosulfates can be produced through photo-oxidation of naphthalene on sulfate particles.[73] If this reaction also occurs for larger PAHs, this could also explain some of polyaromatic compounds. Apparently, there is potential for organosulfates derived polyaromatic compounds as important particle phase constituents.

For CHO-compounds atmospheric generation pathways for linear combined polyaromatic compounds are also known. Phenolic compounds (18% of newly identified CHO-compounds) can react in the aqueous particle phase with OH-radicals leading to the formation of oligomeric compounds among other products.[57, 83] Twenty-one MF of dimeric potential reaction products with two phenyl rings are detected in the SoaF sample as well as in the bulk sample (Table S9). However, only three MF of trimeric reaction products are detected in the bulk. In the SoaF sample three additional ones are detected, like$C_{18}H_{14}O_3$, $C_{18}H_{14}O_4$ and $C_{21}H_{18}O_8$ (Table S9), which were identified as the most abundant products in a laboratory study. [57]If other aromatic compounds are present during this polymerization reaction, a large variety of reactions products is conceivable.

ASSOCIATED CONTENT

Supporting Information

The Supporting Information is available free of charge on the ACS Publications website. Characterization of the Melpitz field site, Sampling parameters, detailed description of the sample preparation and 2D-LC fractionation method, experimental conditions of the FT-ICR-MS measurements, description of the molecular formula assignment and additional molecular properties derived from it, detailed discussion of the calculation of the carbon oxidation state, discussion of the quality control measurements, further discussion on additional compound classes detected in the samples, and additional figures for the distribution of signals in various 2D spaces. Further, a csv-data is provided including all measured signals of the discussed dataset.

Author Information

Corresponding author

* Phone: 49 341 2717 7024. Fax: 49 341 2717 99 7024. E-mail: herrmann@tropos.de.

Author Contributions

The manuscript was written through contributions of all authors and all authors have given approval to the final version of the manuscript

Notes

The authors declare no competing financial interest.

Acknowledgement

This work was funded by the German Research Foundation (DFG) in the project HuCar as PI 1102/4-1 and HE 3086/28-1. The authors are grateful for using the analytical facilities of ProVIS Centre for Chemical Microscopy within the Helmholtz Centre for Environmental Research Leipzig, which is supported by European regional Development Funds (EFRE – Europe funds Saxony) and the Helmholtz Association. Support of the TROPOS ACD labs through EFRE is as well acknowledged. The authors would also like to thank Gerald Spindler and Anke Rödger for providing the filter samples and additional data and Boris Koch for developing and providing the FTICR-MS molecular formula calculation software used in this study. The authors also thank the anonymous reviewers for their helpful criticism and comments.

References

1. Kanakidou, M.; Seinfeld, J. H.; Pandis, S. N.; Barnes, I.; Dentener, F. J.; Facchini, M. C.; Van Dingenen, R.; Ervens, B.; Nenes, A.; Nielsen, C. J.; Swietlicki, E.; Putaud, J. P.; Balkanski, Y.; Fuzzi, S.; Horth, J.; Moortgat, G. K.; Winterhalter, R.; Myhre, C. E. L.; Tsigaridis, K.; Vignati, E.; Stephanou, E. G.; Wilson, J. Organic aerosol and global climate modelling: a review. *Atmos Chem Phys* **2005,** *5*, 1053-1123.

2. Chow, J. C.; Doraiswamy, P.; Watson, J. G.; Antony-Chen, L. W.; Ho, S. S. H.; Sodeman, D. A. Advances in integrated and continuous measurements for particle mass and chemical, composition. *J Air Waste Manage* **2008,** *58*, (2), 141-163.

3. Dinar, E.; Taraniuk, I.; Graber, E. R.; Anttila, T.; Mentel, T. F.; Rudich, Y. Hygroscopic growth of atmospheric and model humic-like substances. *J Geophys Res-Atmos* **2007,** *112*, (D05211).

4. Fors, E. O.; Rissler, J.; Massling, A.; Svenningsson, B.; Andreae, M. O.; Dusek, U.; Frank, G. P.; Hoffer, A.; Bilde, M.; Kiss, G.; Janitsek, S.; Henning, S.; Facchini, M. C.; Decesari, S.;

Swietlicki, E. Hygroscopic properties of Amazonian biomass burning and European background HULIS and investigation of their effects on surface tension with two models linking H-TDMA to CCNC data. *Atmos Chem Phys* **2010,** *10*, (12), 5625-5639.

5. Kristensen, T. B.; Wex, H.; Nekat, B.; Nojgaard, J. K.; van Pinxteren, D.; Lowenthal, D. H.; Mazzoleni, L. R.; Dieckmann, K.; Koch, C. B.; Mentel, T. F.; Herrmann, H.; Hallar, A. G.; Stratmann, F.; Bilde, M. Hygroscopic growth and CCN activity of HULIS from different environments. *J Geophys Res-Atmos* **2012,** *117*, (D22203).

6. Salma, I.; Ocskay, R.; Varga, I.; Maenhaut, W. Surface tension of atmospheric humic-like substances in connection with relaxation, dilution, and solution pH. *J Geophys Res-Atmos* **2006,** *111*, (D23205).

7. Dinar, E.; Taraniuk, I.; Graber, E. R.; Katsman, S.; Moise, T.; Anttila, T.; Mentel, T. F.; Rudich, Y. Cloud Condensation Nuclei properties of model and atmospheric HULIS. *Atmos Chem Phys* **2006,** *6*, 2465-2481.

8. Padro, L. T.; Tkacik, D.; Lathem, T.; Hennigan, C. J.; Sullivan, A. P.; Weber, R. J.; Huey, L. G.; Nenes, A. Investigation of cloud condensation nuclei properties and droplet growth kinetics of the water-soluble aerosol fraction in Mexico City. *J Geophys Res-Atmos* **2010,** *115*, (D09204).

9. Mauderly, J. L.; Chow, J. C. Health effects of organic aerosols. *Inhal Toxicol* **2008,** *20*, (3), 257-288.

10. Baltensperger, U.; Dommen, J.; Alfarra, R.; Duplissy, J.; Gaeggeler, K.; Metzger, A.; Facchini, M. C.; Decesari, S.; Finessi, E.; Reinnig, C.; Schott, M.; Warnke, J.; Hoffmann, T.; Klatzer, B.; Puxbaum, H.; Geiser, M.; Savi, M.; Lang, D.; Kalberer, M.; Geiser, T. Combined determination of the chemical composition and of health effects of secondary organic aerosols: The POLYSOA project. *J Aerosol Med Pulm D* **2008,** *21*, (1), 145-154.

11. IPCC Summary for Policymakers. In *Climate Change 2013: The Physical Science Basis. Contribution of Working Group I to the Fifth Assessment Report of the Intergovernmental Panel on Climate Change*, Stocker, T. F.; Qin, D.; Plattner, G.-K.; Tignor, M.; Allen, S. K.; Boschung, J.; Nauels, A.; Xia, Y.; Bex, V.; Midgley, P. M., Eds. Cambridge University Press: Cambridge, United Kingdom and New York, NY, USA, 2013; pp 1–30.

12. Zheng, G. J.; He, K. B.; Duan, F. K.; Cheng, Y.; Ma, Y. L. Measurement of humic-like substances in aerosols: A review. *Environ Pollut* **2013,** *181*, 301-314.

13. Graber, E. R.; Rudich, Y. Atmospheric HULIS: How humic-like are they? A comprehensive and critical review. *Atmos Chem Phys* **2006,** *6*, 729-753.

14. Havers, N.; Burba, P.; Lambert, J.; Klockow, D. Spectroscopic characterization of humic-like substances in airborne particulate matter. *J Atmos Chem* **1998,** *29*, (1), 45-54.

15. Varga, B.; Kiss, G.; Ganszky, I.; Gelencser, A.; Krivacsy, Z. Isolation of water-soluble organic matter from atmospheric aerosol. *Talanta* **2001,** *55*, (3), 561-572.

16. Duarte, R. M. B. O.; Duarte, A. C. Application of non-ionic solid sorbents (XAD resins) for the isolation and fractionation of water-soluble organic compounds from atmospheric aerosols. *J Atmos Chem* **2005,** *51*, (1), 79-93.

17. Baduel, C.; Voisin, D.; Jaffrezo, J. L. Comparison of analytical methods for Humic Like Substances (HULIS) measurements in atmospheric particles. *Atmos Chem Phys* **2009,** *9*, (16), 5949-5962.

18. Fan, X. J.; Song, J. Z.; Peng, P. A. Comparison of isolation and quantification methods to measure humic-like substances (HULIS) in atmospheric particles. *Atmos Environ* **2012,** *60*, 366-374.

19. Fan, X. J.; Song, J. Z.; Peng, P. A. Comparative study for separation of atmospheric humic-like substance (HULIS) by ENVI-18, HLB, XAD-8 and DEAE sorbents: Elemental composition, FT-IR, H-1 NMR and off-line thermochemolysis with tetramethylammonium hydroxide (TMAH). *Chemosphere* **2013,** *93*, (9), 1710-1719.

20. Sullivan, A. P.; Weber, R. J. Chemical characterization of the ambient organic aerosol soluble in water: 1. Isolation of hydrophobic and hydrophilic fractions with a XAD-8 resin. *J Geophys Res-Atmos* **2006,** *111*, (D05314).

21. Sullivan, A. P.; Weber, R. J. Chemical characterization of the ambient organic aerosol soluble in water: 2. Isolation of acid, neutral, and basic fractions by modified size-exclusion chromatography. *J Geophys Res-Atmos* **2006,** *111*, (D05315).

22. Schmitt-Kopplin, P.; Gelencser, A.; Dabek-Zlotorzynska, E.; Kiss, G.; Hertkorn, N.; Harir, M.; Hong, Y.; Gebefugi, I. Analysis of the Unresolved Organic Fraction in Atmospheric Aerosols with Ultrahigh-Resolution Mass Spectrometry and Nuclear Magnetic Resonance Spectroscopy: Organosulfates As Photochemical Smog Constituents. *Anal Chem* **2010,** *82*, (19), 8017-8026.

23. Mead, R. N.; Felix, J. D.; Avery, G. B.; Kieber, R. J.; Willey, J. D.; Podgorski, D. C. Characterization of CHOS compounds in rainwater from continental and coastal storms by ultrahigh resolution mass spectrometry. *Atmos Environ* **2015,** *105*, 162-168.

24. Zhao, Y.; Hallar, A. G.; Mazzoleni, L. R. Atmospheric organic matter in clouds: exact masses and molecular formula identification using ultrahigh-resolution FT-ICR mass spectrometry. *Atmos Chem Phys* **2013,** *13*, (24), 12343-12362.

25. Cottrell, B. A.; Gonsior, M.; Isabelle, L. M.; Luo, W.; Perraud, V.; McIntire, T. M.; Pankow, J. F.; Schmitt-Kopplin, P.; Cooper, W. J.; Simpson, A. J. A regional study of the seasonal variation in the molecular composition of rainwater. *Atmos Environ* **2013,** *77*, 588-597.

26. Willoughby, A. S.; Wozniak, A. S.; Hatcher, P. G. Detailed Source-Specific Molecular Composition of Ambient Aerosol Organic Matter Using Ultrahigh Resolution Mass Spectrometry and H-1 NMR. *Atmosphere-Basel* **2016,** *7*, (6).

27. Putman, A. L.; Offenberg, J. H.; Fisseha, R.; Kundu, S.; Rahn, T. A.; Mazzoleni, L. R. Ultrahigh-resolution FT-ICR mass spectrometry characterization of alpha-pinene ozonolysis SOA. *Atmos Environ* **2012,** *46*, 164-172.

28. Lin, P.; Rincon, A. G.; Kalberer, M.; Yu, J. Z. Elemental Composition of HULIS in the Pearl River Delta Region, China: Results Inferred from Positive and Negative Electrospray High Resolution Mass Spectrometric Data. *Environ Sci Technol* **2012,** *46*, (14), 7454-7462.

29. Reemtsma, T.; These, A.; Venkatachari, P.; Xia, X. Y.; Hopke, P. K.; Springer, A.; Linscheid, M. Identification of fulvic acids and sulfated and nitrated analogues in atmospheric aerosol by electrospray ionization Fourier transform ion cyclotron resonance mass spectrometry. *Anal Chem* **2006,** *78*, (24), 8299-8304.

30. Marshall, A. G.; Hendrickson, C. L.; Jackson, G. S. Fourier transform ion cyclotron resonance mass spectrometry: A primer. *Mass Spectrom Rev* **1998,** *17*, (1), 1-35.

31. Hawkes, J. A.; Dittmar, T.; Patriarca, C.; Tranvik, L.; Bergquist, J. Evaluation of the Orbitrap Mass Spectrometer for the Molecular Fingerprinting Analysis of Natural Dissolved Organic Matter. *Anal Chem* **2016,** *88*, (15), 7698-7704.

32. Wang, X. K.; Rossignol, S.; Ma, Y.; Yao, L.; Wang, M. Y.; Chen, J. M.; George, C.; Wang, L. Molecular characterization of atmospheric particulate organosulfates in three megacities at the middle and lower reaches of the Yangtze River. *Atmos Chem Phys* **2016,** *16*, (4), 2285-2298.

33. Hockaday, W. C.; Purcell, J. M.; Marshall, A. G.; Baldock, J. A.; Hatcher, P. G. Electrospray and photoionization mass spectrometry for the characterization of organic matter in natural waters: a qualitative assessment. *Limnol Oceanogr-Meth* **2009,** *7*, 81-95.

34. Ohno, T.; Sleighter, R. L.; Hatcher, P. G. Comparative study of organic matter chemical characterization using negative and positive mode electrospray ionization ultrahigh-resolution mass spectrometry. *Anal Bioanal Chem* **2016,** *408*, (10), 2497-2504.

35. Kruve, A.; Leito, I.; Herodes, K. Combating matrix effects in LC/ESI/MS: The extrapolative dilution approach. *Anal Chim Acta* **2009,** *651*, (1), 75-80.

36. Souverain, S.; Rudaz, S.; Veuthey, J. L. Matrix effect in LC-ESI-MS and LC-APCI-MS with off-line and on-line extraction procedures. *J Chromatogr A* **2004,** *1058*, (1-2), 61-66.

37. Stuber, M.; Reemtsma, T. Evaluation of three calibration methods to compensate matrix effects in environmental analysis with LC-ESI-MS. *Anal Bioanal Chem* **2004,** *378*, (4), 910-916.

38. Patriarca, C.; Bergquist, J.; Sjoberg, P. J. R.; Tranvik, L.; Hawkes, J. A. Online HPLC-ESI-HRMS Method for the Analysis and Comparison of Different Dissolved Organic Matter Samples. *Environ Sci Technol* **2018,** *52*, (4), 2091-2099.

39. Wang, K.; Zhang, Y.; Huang, R.-J.; Cao, J.; Hoffmann, T. UHPLC-Orbitrap mass spectrometric characterization of organic aerosol from a central European city (Mainz, Germany) and a Chinese megacity (Beijing). *Atmos Environ* **2018,** *189*, 22-29.

40. Hawkes, J. A.; Patriarca, C.; Sjöberg, P. J. R.; Tranvik, L. J.; Bergquist, J. Extreme isomeric complexity of dissolved organic matter found across aquatic environments. *Limnology and Oceanography Letters* **2018,** *3*, (2), 21-30.

41. Matos, J. T. V.; Freire, S. M. S. C.; Duarte, R. M. B. O.; Duarte, A. C. Profiling Water-Soluble Organic Matter from Urban Aerosols Using Comprehensive Two-Dimensional Liquid Chromatography. *Aerosol Sci Tech* **2015,** *49*, (6), 381-389.

42. Stenson, A. C. Reversed-phase chromatography fractionation tailored to mass spectral characterization of humic substances. *Environ Sci Technol* **2008,** *42*, (6), 2060-2065.

43. Spranger, T.; van Pinxteren, D.; Herrmann, H. Two-Dimensional Offline Chromatographic Fractionation for the Characterization of Humic-Like Substances in Atmospheric Aerosol Particles. *Environ Sci Technol* **2017,** *51*, (9), 5061-5070.

44. Spindler, G.; Brueggemann, E.; Gnauk, T.; Gruner, A.; Mueller, K.; Herrmann, H. A four-year size-segregated characterization study of particles PM10, PM2.5 and PM1 depending on air mass origin at Melpitz. *Atmos Environ* **2010,** *44*, (2), 164-173.

45. Cook, R. D.; Lin, Y. H.; Peng, Z. Y.; Boone, E.; Chu, R. K.; Dukett, J. E.; Gunsch, M. J.; Zhang, W. L.; Tolic, N.; Laskin, A.; Pratt, K. A. Biogenic, urban, and wildfire influences on the molecular composition of dissolved organic compounds in cloud water. *Atmos Chem Phys* **2017,** *17*, (24), 15167-15180.

46. Koch, B. P.; Dittmar, T.; Witt, M.; Kattner, G. Fundamentals of molecular formula assignment to ultrahigh resolution mass data of natural organic matter. *Anal. Chem.* **2007,** *79*, (4), 1758-1763.

47. Lechtenfeld, O. J.; Hertkorn, N.; Shen, Y.; Witt, M.; Benner, R. Marine sequestration of carbon in bacterial metabolites. *Nat Commun* **2015,** *6*, 6711.

48. Duporte, G.; Riva, M.; Parshintsev, J.; Heikkinen, E.; Barreira, L. M. F.; Myllys, N.; Heikkinen, L.; Hartonen, K.; Kulmala, M.; Ehn, M.; Riekkola, M. L. Chemical Characterization of Gas- and Particle-Phase Products from the Ozonolysis of alpha-Pinene in the Presence of Dimethylamine. *Environ Sci Technol* **2017,** *51*, (10), 5602-5610.

49. Faxon, C.; Hammes, J.; Le Breton, M.; Pathak, R. K.; Hallquist, M. Characterization of organic nitrate constituents of secondary organic aerosol (SOA) from nitrate-radical-initiated oxidation of limonene using high-resolution chemical ionization mass spectrometry. *Atmos Chem Phys* **2018,** *18*, (8), 5467-5481.

50. Walhout, E. Q.; Dorn, S. E.; Martens, J.; Berden, G.; Oomens, J.; Cheong, P. H. Y.; Kroll, J. H.; O'Brien, R. E. Infrared Ion Spectroscopy of Environmental Organic Mixtures: Probing the Composition of alpha-Pinene Secondary Organic Aerosol. *Environ Sci Technol* **2019,** *53*, (13), 7604-7612.

51. Willoughby, A. S.; Wozniak, A. S.; Hatcher, P. G. A molecular-level approach for characterizing water-insoluble components of ambient organic aerosol particulates using ultrahigh-resolution mass spectrometry. *Atmos Chem Phys* **2014,** *14*, (18), 10299-10314.

52. Altieri, K. E.; Turpin, B. J.; Seitzinger, S. P. Composition of Dissolved Organic Nitrogen in Continental Precipitation Investigated by Ultra-High Resolution FT-ICR Mass Spectrometry. *Environ Sci Technol* **2009,** *43*, (18), 6950-6955.

53. Samburova, V.; Hallar, A. G.; Mazzoleni, L. R.; Saranjampour, P.; Lowenthal, D.; Kohl, S. D.; Zielinska, B. Composition of water-soluble organic carbon in non-urban atmospheric aerosol collected at the Storm Peak Laboratory. *Environ Chem* **2013,** *10*, (5), 370-380.

54. Yassine, M. M.; Harir, M.; Dabek-Zlotorzynska, E.; Schmitt-Kopplin, P. Structural characterization of organic aerosol using Fourier transform ion cyclotron resonance mass spectrometry: Aromaticity equivalent approach. *Rapid Commun Mass Sp* **2014,** *28*, (22), 2445-2454.

55. Kroll, J. H.; Donahue, N. M.; Jimenez, J. L.; Kessler, S. H.; Canagaratna, M. R.; Wilson, K. R.; Altieri, K. E.; Mazzoleni, L. R.; Wozniak, A. S.; Bluhm, H.; Mysak, E. R.; Smith, J. D.; Kolb, C. E.; Worsnop, D. R. Carbon oxidation state as a metric for describing the chemistry of atmospheric organic aerosol. *Nat Chem* **2011,** *3*, (2), 133-139.

56. Aiken, A. C.; Decarlo, P. F.; Kroll, J. H.; Worsnop, D. R.; Huffman, J. A.; Docherty, K. S.; Ulbrich, I. M.; Mohr, C.; Kimmel, J. R.; Sueper, D.; Sun, Y.; Zhang, Q.; Trimborn, A.; Northway, M.; Ziemann, P. J.; Canagaratna, M. R.; Onasch, T. B.; Alfarra, M. R.; Prevot, A. S.

H.; Dommen, J.; Duplissy, J.; Metzger, A.; Baltensperger, U.; Jimenez, J. L. O/C and OM/OC ratios of primary, secondary, and ambient organic aerosols with high-resolution time-of-flight aerosol mass spectrometry. *Environ Sci Technol* **2008,** *42*, (12), 4478-4485.

57. Yu, L.; Smith, J.; Laskin, A.; George, K. M.; Anastasio, C.; Laskin, J.; Dillner, A. M.; Zhang, Q. Molecular transformations of phenolic SOA during photochemical aging in the aqueous phase: competition among oligomerization, functionalization, and fragmentation. *Atmos Chem Phys* **2016,** *16*, (7), 4511-4527.

58. Kim, S.; Kramer, R. W.; Hatcher, P. G. Graphical method for analysis of ultrahigh-resolution broadband mass spectra of natural organic matter, the van Krevelen diagram. *Anal Chem* **2003,** *75*, (20), 5336-5344.

59. O'Brien, R. E.; Laskin, A.; Laskin, J.; Rubitschun, C. L.; Surratt, J. D.; Goldstein, A. H. Molecular characterization of S- and N-containing organic constituents in ambient aerosols by negative ion mode high-resolution Nanospray Desorption Electrospray Ionization Mass Spectrometry: CalNex 2010 field study. *J Geophys Res-Atmos* **2014,** *119*, (22), 12706-12720.

60. Dzepina, K.; Mazzoleni, C.; Fialho, P.; China, S.; Zhang, B.; Owen, R. C.; Helmig, D.; Hueber, J.; Kumar, S.; Perlinger, J. A.; Kramer, L. J.; Dziobak, M. P.; Ampadu, M. T.; Olsen, S.; Wuebbles, D. J.; Mazzoleni, L. R. Molecular characterization of free tropospheric aerosol collected at the Pico Mountain Observatory: a case study with a long-range transported biomass burning plume. *Atmos Chem Phys* **2015,** *15*, (9), 5047-5068.

61. Kourtchev, I.; Fuller, S. J.; Giorio, C.; Healy, R. M.; Wilson, E.; O'Connor, I.; Wenger, J. C.; McLeod, M.; Aalto, J.; Ruuskanen, T. M.; Maenhaut, W.; Jones, R.; Venables, D. S.; Sodeau, J. R.; Kulmala, M.; Kalberer, M. Molecular composition of biogenic secondary organic aerosols using ultrahigh-resolution mass spectrometry: comparing laboratory and field studies. *Atmos Chem Phys* **2014,** *14*, (4), 2155-2167.

62. Koch, B. P.; Ludwichowski, K. U.; Kattner, G.; Dittmar, T.; Witt, M. Advanced characterization of marine dissolved organic matter by combining reversed-phase liquid chromatography and FT-ICR-MS. *Mar Chem* **2008,** *111*, (3-4), 233-241.

63. Reemtsma, T.; These, A.; Springer, A.; Linscheid, M. Fulvic acids as transition state of organic matter: Indications from high resolution mass spectrometry. *Environ Sci Technol* **2006,** *40*, (19), 5839-5845.

64. Zhang, J. Y.; Dransfield, T.; Donahue, N. M. On the mechanism for nitrate formation via the peroxy radical plus NO reaction. *J Phys Chem A* **2004,** *108*, (42), 9082-9095.

65. Ng, N. L.; Brown, S. S.; Archibald, A. T.; Atlas, E.; Cohen, R. C.; Crowley, J. N.; Day, D. A.; Donahue, N. M.; Fry, J. L.; Fuchs, H.; Griffin, R. J.; Guzman, M. I.; Herrmann, H.; Hodzic, A.; Iinuma, Y.; Jimenez, J. L.; Kiendler-Scharr, A.; Lee, B. H.; Luecken, D. J.; Mao, J. Q.; McLaren, R.; Mutzel, A.; Osthoff, H. D.; Ouyang, B.; Picquet-Varrault, B.; Platt, U.; Pye, H. O. T.; Rudich, Y.; Schwantes, R. H.; Shiraiwa, M.; Stutz, J.; Thornton, J. A.; Tilgner, A.; Williams, B. J.; Zaveri, R. A. Nitrate radicals and biogenic volatile organic compounds: oxidation, mechanisms, and organic aerosol. *Atmos Chem Phys* **2017,** *17*, (3), 2103-2162.

66. Liu, S.; Shilling, J. E.; Song, C.; Hiranuma, N.; Zaveri, R. A.; Russell, L. M. Hydrolysis of Organonitrate Functional Groups in Aerosol Particles. *Aerosol Sci Tech* **2012,** *46*, (12), 1359-1369.

67. Hughey, C. A.; Hendrickson, C. L.; Rodgers, R. P.; Marshall, A. G.; Qian, K. N. Kendrick mass defect spectrum: A compact visual analysis for ultrahigh-resolution broadband mass spectra. *Anal Chem* **2001,** *73*, (19), 4676-4681.

68. Tao, S.; Lu, X.; Levac, N.; Bateman, A. P.; Nguyen, T. B.; Bones, D. L.; Nizkorodov, S. A.; Laskin, J.; Laskin, A.; Yang, X. Molecular Characterization of Organosulfates in Organic Aerosols from Shanghai and Los Angeles Urban Areas by Nanospray-Desorption Electrospray Ionization High-Resolution Mass Spectrometry. *Environ Sci Technol* **2014,** *48*, (18), 10993-11001.

69. Iinuma, Y.; Muller, C.; Berndt, T.; Böge, O.; Claeys, M.; Herrmann, H. Evidence for the existence of organosulfates from beta-pinene ozonolysis in ambient secondary organic aerosol. *Environ Sci Technol* **2007,** *41*, (19), 6678-6683.

70. Iinuma, Y.; Muller, C.; Böge, O.; Gnauk, T.; Herrmann, H. The formation of organic sulfate esters in the limonene ozonolysis secondary organic aerosol (SOA) under acidic conditions. *Atmos Environ* **2007,** *41*, (27), 5571-5583.

71. Surratt, J. D.; Gomez-Gonzalez, Y.; Chan, A. W. H.; Vermeylen, R.; Shahgholi, M.; Kleindienst, T. E.; Edney, E. O.; Offenberg, J. H.; Lewandowski, M.; Jaoui, M.; Maenhaut, W.; Claeys, M.; Flagan, R. C.; Seinfeld, J. H. Organosulfate formation in biogenic secondary organic aerosol. *J Phys Chem A* **2008,** *112*, (36), 8345-8378.

72. Surratt, J. D.; Kroll, J. H.; Kleindienst, T. E.; Edney, E. O.; Claeys, M.; Sorooshian, A.; Ng, N. L.; Offenberg, J. H.; Lewandowski, M.; Jaoui, M.; Flagan, R. C.; Seinfeld, J. H. Evidence for organosulfates in secondary organic aerosol. *Environ Sci Technol* **2007,** *41*, (2), 517-527.

73. Riva, M.; Tomaz, S.; Cui, T. Q.; Lin, Y. H.; Perraudin, E.; Gold, A.; Stone, E. A.; Villenave, E.; Surratt, J. D. Evidence for an Unrecognized Secondary Anthropogenic Source of Organosulfates and Sulfonates: Gas-Phase Oxidation of Polycyclic Aromatic Hydrocarbons in the Presence of Sulfate Aerosol. *Environ Sci Technol* **2015,** *49*, (11), 6654-6664.

74. Raeke, J.; Lechtenfeld, O. J.; Seiwert, B.; Meier, T.; Riemenschneider, C.; Reemtsma, T. Photochemically Induced Bound Residue Formation of Carbamazepine with Dissolved Organic Matter. *Environ Sci Technol* **2017,** *51*, (10), 5523-5530.

75. Minerath, E. C.; Elrod, M. J. Assessing the Potential for Diol and Hydroxy Sulfate Ester Formation from the Reaction of Epoxides in Tropospheric Aerosols. *Environ Sci Technol* **2009,** *43*, (5), 1386-1392.

76. Lin, P.; Yu, J. Z.; Engling, G.; Kalberer, M. Organosulfates in Humic-like Substance Fraction Isolated from Aerosols at Seven Locations in East Asia: A Study by Ultra-High-Resolution Mass Spectrometry. *Environ Sci Technol* **2012,** *46*, (24), 13118-13127.

77. Hu, K. S.; Darer, A. I.; Elrod, M. J. Thermodynamics and kinetics of the hydrolysis of atmospherically relevant organonitrates and organosulfates. *Atmos Chem Phys* **2011,** *11*, (16), 8307-8320.

78. Passananti, M.; Kong, L. D.; Shang, J.; Dupart, Y.; Perrier, S.; Chen, J. M.; Donaldson, D. J.; George, C. Organosulfate Formation through the Heterogeneous Reaction of Sulfur Dioxide with Unsaturated Fatty Acids and Long-Chain Alkenes. *Angew Chem Int Edit* **2016,** *55*, (35), 10336-10339.

79. Lammel, G. Polycyclic Aromatic Compounds in the Atmosphere - A Review Identifying Research Needs. *Polycycl Aromat Comp* **2015,** *35*, (2-4), 316-329.

80. Fuzzi, S.; Andreae, M. O.; Huebert, B. J.; Kulmala, M.; Bond, T. C.; Boy, M.; Doherty, S. J.; Guenther, A.; Kanakidou, M.; Kawamura, K.; Kerminen, V. M.; Lohmann, U.; Russell, L. M.; Poschl, U. Critical assessment of the current state of scientific knowledge, terminology, and research needs concerning the role of organic aerosols in the atmosphere, climate, and global change. *Atmos Chem Phys* **2006,** *6*, 2017-2038.

81. Hoffmann, E. H.; Tilgner, A.; Wolke, R.; Böge, O.; Walter, A.; Herrmann, H. Oxidation of substituted aromatic hydrocarbons in the tropospheric aqueous phase: kinetic mechanism development and modelling. *Phys Chem Chem Phys* **2018,** *20*, (16), 10960-10977.

82. Teich, M.; van Pinxteren, D.; Kecorius, S.; Wang, Z. B.; Herrmann, H. First Quantification of Imidazoles in Ambient Aerosol Particles: Potential Photosensitizers, Brown Carbon Constituents, and Hazardous Components. *Environ Sci Technol* **2016,** *50*, (3), 1166-1173.

83. Sun, Y. L.; Zhang, Q.; Anastasio, C.; Sun, J. Insights into secondary organic aerosol formed via aqueous-phase reactions of phenolic compounds based on high resolution mass spectrometry. *Atmos Chem Phys* **2010,** *10*, (10), 4809-4822.

Toc art:

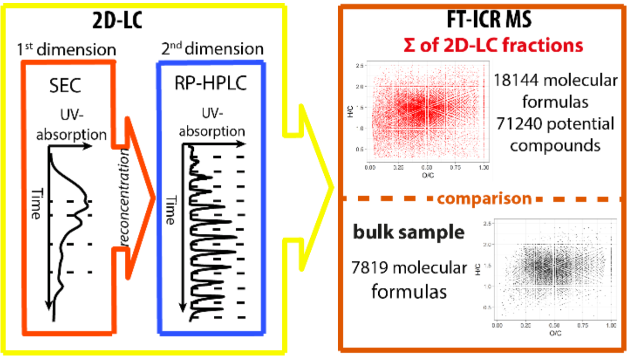
2D-LC
1st dimension
SEC
UV-absorption
Time
reconcentration
2nd dimension
RP-HPLC
UV-absorption
Time
FT-ICR MS
Σ of 2D-LC fractions
H/C
O/C
0.00
0.25
0.50
0.75
1.00
0.5
1.0
1.5
2.0
2.5
18144 molecular formulas
71240 potential compounds
comparison
bulk sample
7819 molecular formulas